Waterflooding in Gordon Sandstone Formation – Taylorstown Field

during the Period 05/15/2001 to 11/30/2002

By

Mario Farías, José Zaghloul, Turgay Ertekin, and Robert Watson (PNGE – PSU)
Terry Pegula, and William Fustos (East Resources Inc.)

The Pennsylvania State University
The College of Earth and Mineral Science
The Department of Energy and Geo-Enviromental Engineering
The Energy Institute
East Resources Incorporated

April 20, 2003

Work Performed Under Prime Award No. DE-FC26-00NT41025
Subcontract No. 2040-TPSU-DOE-1025

For
U.S. Department of Energy
National Energy Technology Laboratory
P.O. Box 10940
Pittsburgh, Pennsylvania 15236

By
The Pennsylvania State University
The College of Earth and Mineral Science
The Department of Energy and Geo-Enviromental Engineering
The Energy Institute
East Resources Incorporated

PROJECT TITLE

Waterflooding in Gordon sandstone formation – Taylorstown field

By

Mario Farías, José Zaghloul, Turgay Ertekin, and Robert Watson (PNGE – PSU)
Terry Pegula, and William Fustos (East Resources Inc.)

Date
April 20, 2003

Work Performed Under Grant No. *(DE-FC26-00NT41025)*
Subcontract No. *(2038-TPSU-DOE-1025)*
Subcontract No. *(2040-TPSU-DOE-1025)*

For
U.S. Department of Energy

By
The Pennsylvania State University.
The College of Earth and Mineral Science.
The Department of Energy and Geo-Enviromental Engineering.
The Energy Institute.
East Resources Incorporated.

DISCLAIMER

ABSTRACT

The Appalachian Region contains hundreds of oil fields that were developed during the late 1800's and/or early 1900's. These fields contain oil reserves that may be recovered using secondary recovery methods such as waterflooding. Technical and economic evaluation of these fields for these capital-intensive operations requires in-depth engineering studies that usually include a field-scale computer model. However, the data needed for building such models are lacking given that modern tools for formation evaluation were not available when these fields were developed (early 1900's).

The objectives of this study are to develop techniques for simulating these first-generation oil fields and to analyze the dynamic nature of near-wellbore damage of injection and production wells. These techniques are demonstrated for the Taylorstown field located in Washington County, PA. This reservoir (Upper Devonian Gordon Sandstone), which is currently undergoing waterflooding, is used as case study. Reservoir model of the field was developed and used to study the dynamic skin damage effect.

This study describes the approach, and protocol employed to characterize and build the computer model of the field in spite of the sparse data sets. The protocol utilizes a systematic approach to complete the history matching, which proved to be effective in understanding the behavior of the reservoir under study. The results obtained provide the operators of the Appalachian basin with a tool to characterize, initialize and perform computer simulation studies of any of the hundreds of reservoirs found in the basin.

It was concluded that the change in well-bore damage with time in waterflooding operations might result from the types of fluids injected. In the Washington-Taylorstown field, it appears that the major factor was a history of gas injection and water injection using water obtained from coalmine operations and gas fields. This resulted in the presence of mobile emulsions and suspended solids that reduced injectivity and productivity of injection and production wells, respectively.

TABLE OF CONTENTS

LIST OF FIGURES

LIST OF TABLES

1.0 INTRODUCTION

The goal of reservoir engineering and its attendant studies is to maximize oil recovery from the subject reservoir. During the primary production phase, it is the management of the natural energy of the reservoir that maximizes the production. However, continued production at an economic level typically requires implementation of secondary recovery technologies such as waterflooding.

With waterflooding, collateral effects come into the picture since the reservoir is being perturbed. This study presents guideline for the development of reservoir models where "insufficient" data are available and concentrates on the effects of water injection on the rock matrix, specifically skin damage. Skin damage can be caused by a variety of external or internal mechanisms. These mechanisms can include damage that result from fluid invasion during the drilling operation. It can also result from the impact of fluid injection and or production on the reservoir rock. Skin damage is quantified by dimensionless pressure drop that is referred to as skin factor.

The purpose of this study is to investigate the skin factor as a time dependent function, in other words, an investigation of dynamic skin. In order to achieve this objective, numerical reservoir simulation is used as the platform for the analysis of the reservoir performance. Data obtained from the reservoirs undergoing waterflooding are used to support the study.

Numerical reservoir simulation is a tool widely employed by reservoir engineers to understand the past and present behavior of a reservoir. It is also used to estimate rock and fluid properties, and for predicting future performance of a field under various operating conditions. In reservoir simulation, rock and fluid properties are characterized and used to build a mathematical model. This model is then used to solve the governing partial differential equations that describe the movement of the different phases in the reservoir, and thereby mimic the time-dependent variation of pressure and production rates.

During the construction of the model, a matching of the historical data and simulation results is used to adjust the values of the properties assigned, and verify the boundary conditions of the model. A "good" qualitative and quantitative match validates the accuracy of the model, and confirms the ability of the

mathematical model to recreate the complex behavior of the reservoir. Using numerical reservoir simulation, engineers can forecast production of oil, water and gas, estimate the reserves and evaluate the viability of the project under of various operating scenarios.

1.1 Background

To accomplish the study of dynamic skin, data from ongoing field operations were used. The data were from the Gordon sandstone formation found in the Appalachian Basin. The Gordon sand belongs to the Venango group of the Upper Devonian age and received its name in 1885 when discovered by drilling operations on the Gordon farm in Washington, Pennsylvania.

Among the most predominant properties that characterize the sandstone at this location are: 1) the depth at which it is found (between 1500-ft and 3000-ft); 2) the permeability ranges (from 90-md to 200-md); and 3) the average porosity value of approximately 20 percent. Values out of these ranges could generally be found in any of the wells penetrating this formation (*Harper, 1987 and Lytle, 1950*).

The area of interest related to the study is located in Washington County, southwest Pennsylvania, where the field of Washington-Taylorstown is located. The field produces from the Gordon sand formation and is one of the many fields found in Pennsylvania, Ohio and West Virginia that have the potential for waterflooding.

Fields penetrating the Gordon formation were discovered in the late 1800s and at the beginning of the 20th century. During the early development stage of the fields, primary production was the principal mechanism for oil production. However, this primary production ended by the middle of the century because the reservoir drive mechanism was depleted. It was estimated that approximately 10 to 25 percent of the original oil in place had been recovered. Therefore, alternative recovery methods have been studied to keep these stripper well reservoirs economically profitable (*Cardwell, 1978*). Stimulation and secondary oil recovery projects were applied to different areas of the reservoir, with varying degrees of success. Gas

injection and waterflooding were the most widely secondary recovery methods even though air injection has also been practiced.

It is postulated that the implementation of these secondary recovery projects has resulted in significant damage in the wellbore and the adjoining reservoir. This study seeks to use the field data to quantify the dynamics of skin damage.

1.2 Problem Statement

To simulate and analyze the behavior of a reservoir it is often necessary to develop a field scale computer model. However, data of the type necessary for building the model are often quite sparse. The lack of data is often the case with reservoirs that were developed before the availability of modern tools for formation evaluation, or when data from the early stages of the development of the fields are not available. Given this problem, this study focuses on detailing the efforts and techniques used to develop a model for reservoirs with sparse data sets. Also, this study analyzes several factors to improve the history matching process in fields with sparse data sets.

The skin factor is the representation of a damaged or stimulated wellbore. Skin damage is present from the time a well is drilled, and then completed. It is present during the entire life of the well whether the well is in operation for production or injection purposes.

Although skin effect has been the subject of numerous investigations, e.g. Fetkcovich (1973), Tippie et al. (1974), Blacker (1982) and Hansen et al. (2002), the dynamic nature of the phenomenon has not been thoroughly investigated. Dynamic skin is influenced by a variety of parameters that cause the productivity index of the well to vary. It is well understood that operating conditions are not always the same. For example, the reservoir conditions may change with oil production and fluid injection rates may vary with well stimulation and/or mobilization of suspended particles by the injected fluid. These changes and their impact on the wellbore (skin damage) must be considered in conducting a reservoir analysis.

Analysis of the impact of dynamic skin on production and injection rates is the focus of this investigation. To achieve these objectives, the Washington-Taylorstown field is used as the case study. The results of these analyses are used to provide insight concerning the dynamic skin.

The representation of the dynamic skin effect is made with numerical reservoir simulation. A commercial black oil model simulator (Eclipse 100) is used as the tool to pursue the principal objective of this study. The methodology used to develop the model is the history matching process, which when coupled with current field operating reports confirm the veracity of this approach.

2.0 CHARACTERIZATION OF THE RESERVOIR

The Gordon sandstone formation is located in the Appalachian Basin. This formation is of Venango group in the Upper Devonian age. Primary production from these fields occurred during the late 1800's and early 1900's. With depletion, remaining oil recovery will require implementation of a secondary recovery method such as waterflooding.

The case study presented in this research is the Washington-Taylorstown field located in Pennsylvania. This field is of the Gordon sandstone formation. Specific characteristics of the Gordon sandstone at Washington-Taylorstown are not available. Given this lack of data concerning reservoir properties, average values are generally used. These "rule of thumb" values are based on the few cores that have been obtained from wells penetrating the Gordon sandstone and from historical records available from the State Geological Surveys. The data include peculiarities with respect to deposition and/or saturation distribution. The fluid properties are also shown in a section of this chapter. Oil produced from both of the fields appear to be similar in terms of viscosity, API gravity and density.

2.1 Washington-Taylorstown field

This reservoir is located in southwestern Pennsylvania, specifically in Washington County, and covers an area of 4858 acres. The drilling for oil and gas in this area started as early as 1861, but it was not until 1885 that the Washington-Taylorstown field was discovered and production began (*Harper, 1987*).

In the study area, the top of the structure is found at an average depth of 1330-ft below datum level (sea level). The depth of field trends south to north with the southern portion of the field being 70-ft deeper than the northern portion. As a consequence, the rate of change of the gravitational forces along the north-south axis of the field is 1-ft per 240-ft of length. The difference in depth between the east and the west side of the reservoir is approximately 20-ft. In terms of the gravitational effect on fluid flow, it would appear

that the principal impact is felt in the north-south direction. It is also noted that the reservoir properties such as thickness and absolute permeability vary along this axis.

The well wireline logs confirmed the gross thickness and net thickness of the reservoir provided by the isopach maps. These properties average 25-ft and 9-ft respectively. Higher values of both gross thickness and net thickness are found along the main axis in the north-south direction and tend to thin out toward the edges of the reservoir. As a consequence the reservoir shape is characterized as a half pipe that runs in the north-south direction (see Figure 2.1).

The distribution of porosity in the reservoir varies slightly, with maximum values lying along the centerline of the north-south axis. The overall porosity of the field averages 20 % with maximum values of 45 % at the centerline of the reservoir and 4 % at the boundaries.

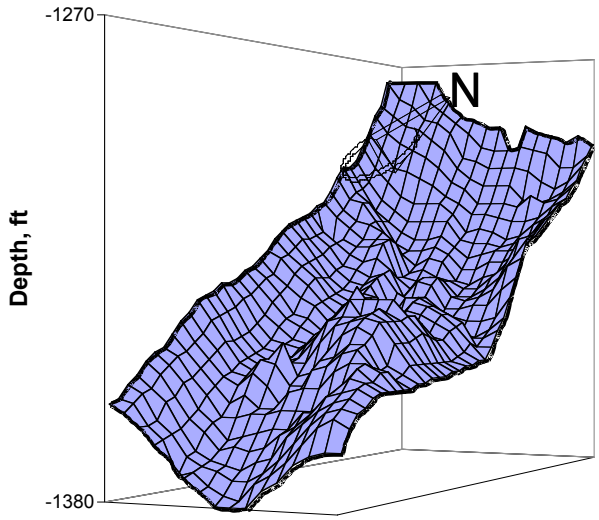

Figure 2.1: Washington-Taylorstown field, bottom of the formation.

One of the most important properties in any reservoir characterization study is the permeability. The permeability is considered as an anisotropic property. The directional distribution has the principal flow

flow trend in the northeast-southwest direction, i.e. the axis running along the injection line-drive. The axis in the northwest-southeast direction represents the secondary flow direction.

The average permeability in the northeast-southwest direction is 130 md and in the northwest-southeast direction, the average permeability is 110 md. Two regions, one on the northeastern portion and the other in the southwestern portion of the field, have permeability values as high as 250 md and 180 md, respectively (Figure 2.2). The previously referred values of directional permeability were obtained from the validation of the computer model, after the history matching process was achieved.

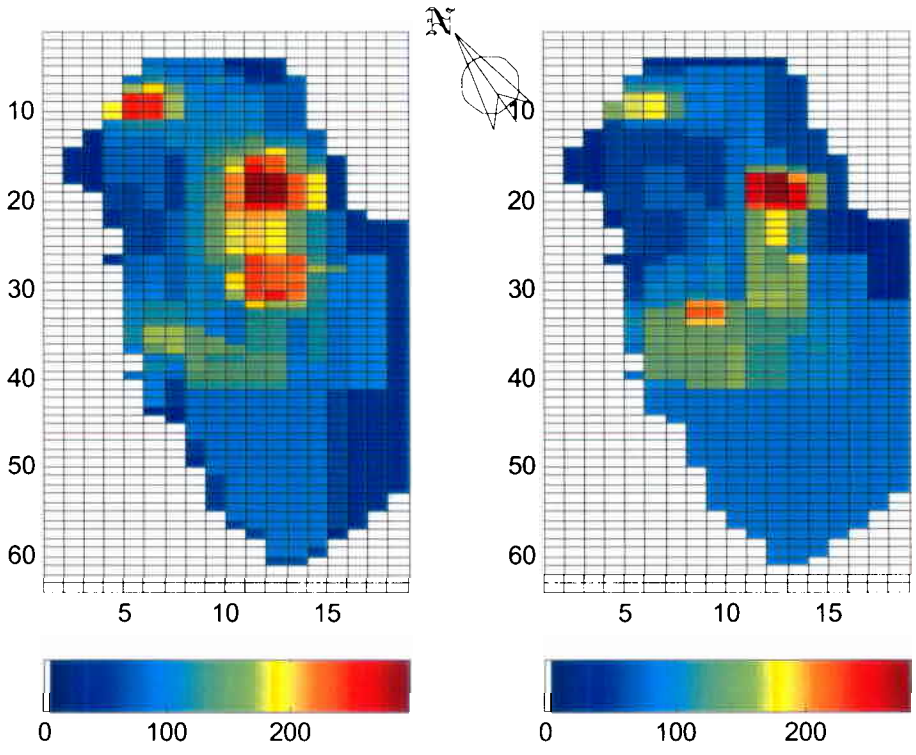

Figure 2.2: Washington-Taylorstown field isoperm maps, directional permeability in the NW-SE (left) and NE-SW (right) directions.

Other properties necessary for the reservoir analysis are saturation of the phases and their distribution. In the case of gas saturation, the operator provided a map of the unit indicating the distribution of the gas saturation. Geologist using values of gas saturation obtained from neutron logs developed the map. The map indicates that the gas saturation toward the southern portion of the reservoir is approximately 10 %. The gas saturation values increase in the center region to approximately 20 % to 30 % and to 50 % to 60 % in the northern region. The water saturation distribution was estimated from resistivity logs obtained from injection wells. From these logs, initial water saturation averages 25 %. The oil saturation considering the variation of water and gas saturations varies from 25 % in the northern area to 70 % in the south.

Using the distribution of phase saturations and reservoir properties (net pay and porosity) it was estimated that approximately 23 MMbbl of oil and 8 MMbbl of gas are contained in the reservoir. These calculations are based on conditions as of 1982.

2.1.1 Washington-Taylorstown field production history

As previously mentioned, the production of the Washington-Taylorstown field started as early as 1885 with 90 barrels of oil per day well. By the end of the century, production from this field was almost 4500 BOPD. However, by 1940, 50 % of all wells to that point in time were inactive.

By today's standards these remaining wells are considered to be stripper wells and are marginally economic. Additional hydrocarbon production would require the implementation of a secondary recovery technique such as waterflooding.

At the present, the field consists of 13 active production wells located east and west of the injection line drive; 6 to the west, 6 to the east and 1 south of the injection line-drive. A map containing the locations of the wells is shown in Figure 2.3. Oil production from the unit started in 1997 with J. Hodgens Sr. 6 well. This well was the sole producer until February 1999 when the drilling of additional wells began. Drilling continued until April 2000. For the purpose of the study, production is considered to

have continued until January 2002. The field has produced approximately 60 Mbbl of oil and 67 Mbbl of water during 6 years of water injection. Figure 2.4 contains a plot of cumulative production of oil and water from the field.

By the second half of 1999, the field experienced an increase in cumulative oil production. It went from 3 Mbbl during the first 2 years to approximately 7.9 Mbbl during the next 6 months. At the same time and 3.5 years after the water injection, cumulative water production increased from approximately 400 bbl to almost 8 Mbbl.

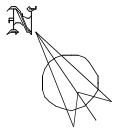

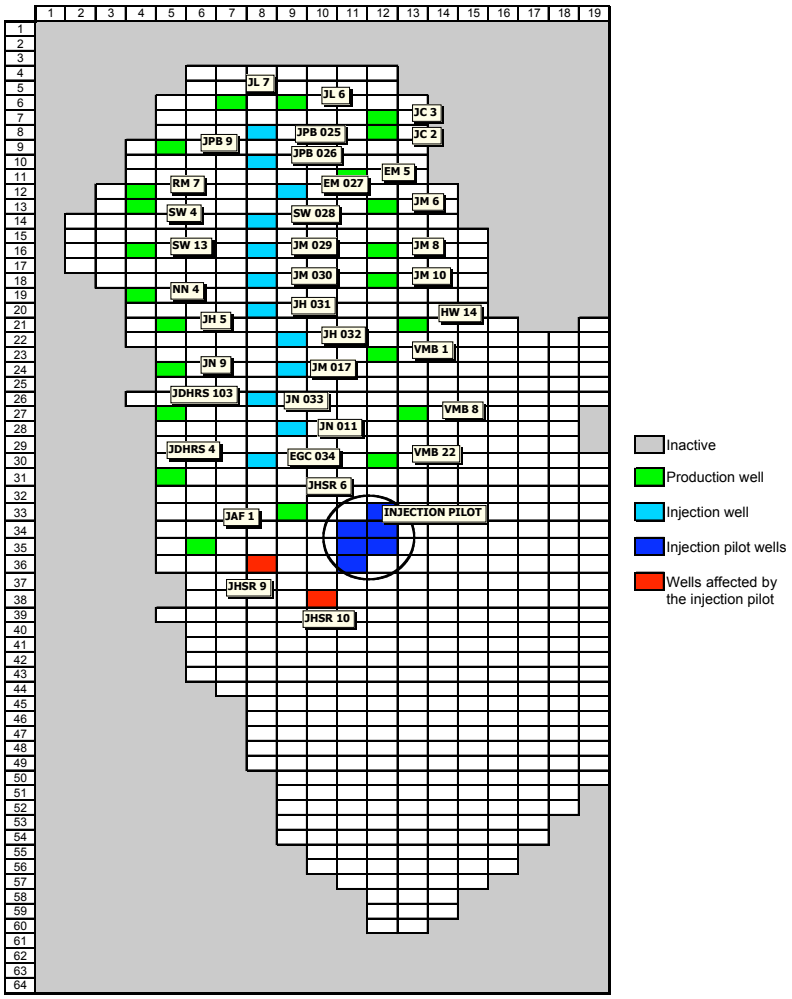

Figure 2.3: Washington-Taylorstown field, location of the active production and injection wells.

This increase in the crude and water production is believed to coincide with the arrival of the oil bank. Interestingly, the J.A. Flack 1 well, the largest cumulative oil producer in the unit, produced this oil during this six month period. At present, production is realized from 5 of the 13 production wells. These are the J.A. Flack 1, V.M Blayney 1, V.M Blayney 8, V.M Blayney 22 and J.P. Bigham 9. This field was a primary producer of oil, gas and water, but only data for the production of the liquids (oil and water) have been collected. The resulting uncertainty with respect to initial reservoir content could not be avoided and resulted in the use of estimates with respect to initial reservoir conditions.

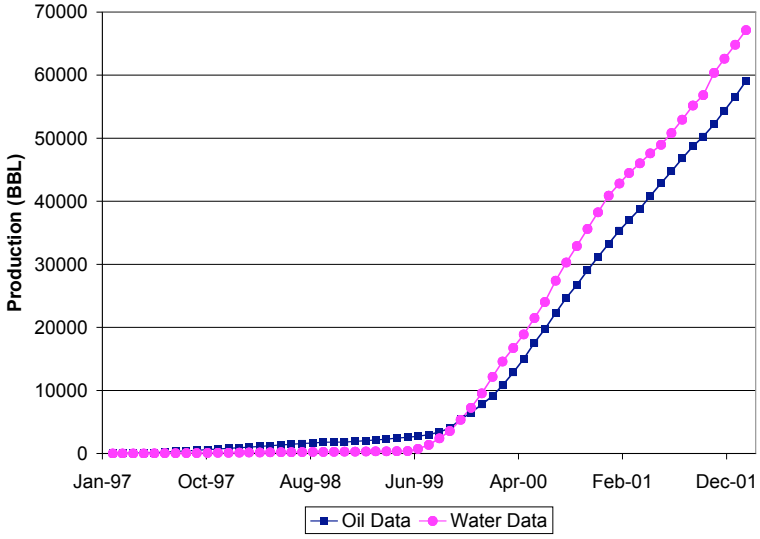

Figure 2.4: Washington-Taylorstown field, cumulative water and oil production.

2.1.2 Washington-Taylorstown field secondary recovery project

Enhanced recovery efforts of the Gordon sandstone have been undertaken almost since its discovery. These efforts took the form of re-injecting the gas that was collected from the gas-oil-water production stream. Field records of these projects are not available and only literature citations of these activities are available from State Geological Surveys bulletins. The first recorded instance of secondary recovery in the Gordon formation was in 1923, when gas drive or repressuring yielded oil recoveries as high as 100 bbl per acre-foot. By 1967, 14 gas injection projects were underway in this field (Harper, 1987), but only one of them took place in the unit studied. For the purposes of this study, gas injection was considered and tuning of the reservoir model incorporated its impact. A more rigorous treatment of its impact could not be implemented due to the lack of available historical data.

During February 1982, a waterflood injection pilot was initiated. It consisted of two contiguous five-spot patterns located in the southeastern portion of the unit. Its location is shown on Figure 2.3, and pilot project lasted almost 7 years. During the 7 years period, 1.2 MM bbl of water was injected into the

reservoir. The effect of this water injection was realized in two wells that are located outside the injection pilot pattern. These wells are the J. Hodgens 9 and J. Hodgens 10, and are located about 1000-ft to the west of the pilot. The production from these two wells was comparable to that from the wells located in the water flood injection pilot area that produced 6.4 Mbbl of oil.

Other implications of the pilot project are:

1. The injection water impacted the performance of the reservoir by altering the saturation distribution in the southern portion of the unit.
2. The pilot proved that the unit's reservoir possesses the petrographic characteristics necessary to sustain a waterflooding project.

In March of 1996, the unit-scale water injection project began. The waterflooding project consisted of 11 injection wells located in a line-drive pattern (see Figure 2.3). The initial injection rate was 4500 bbl/d of water and declined to approximately 800 bbl/d with a cumulative volume injected of approximately 5 MMbbl (see Figure 2.5). The water injected was initially from unconventional sources of water such as coalmine water and formation brine. By December 1999, fresh water injection from a municipal water company started. The fresh water is treated with chemicals to reduce its adverse impact on formation clays (clay swelling).

The locations of the injection wells are toward the center of the reservoir, where the properties of the sand are the most favorable to the process, i.e. the thickness of the reservoir is the greatest and the formation is the deepest (higher injection pressures). The principal disadvantage of this pattern design is that distance between the injection and production wells is large, and consequently the flood front requires additional time to affect the production wells and the swept oil must be displaced a longer distance to the producing well. Also, producing wells are generally located where the formation is the thinnest, which is toward the eastern and western flanks of the reservoir. Coincidental to movement of water towards the flanks of the reservoir, resistance to its flow increases. This is expected given that as the formation thins, rock properties such as permeability and porosity decrease.

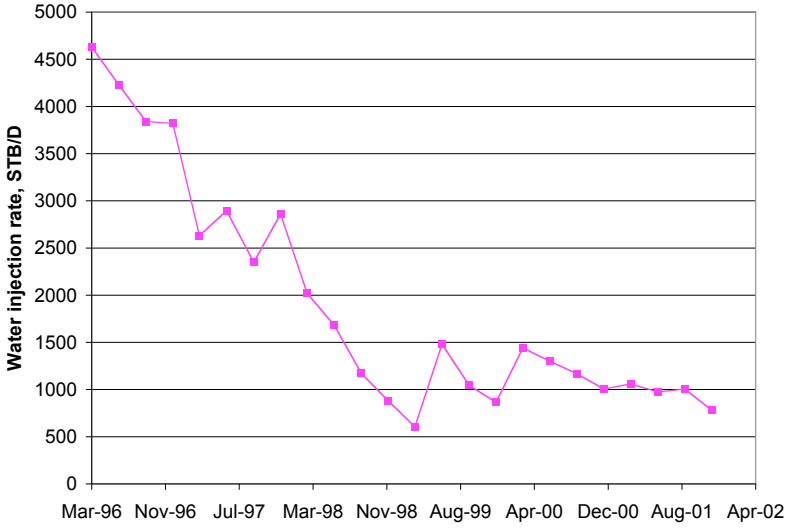

Figure 2.5: Washington-Taylorstown field, total water injection rate.

2.2 Fluid properties

Due to the lack of information about the reservoir fluid properties, several correlations and assumptions were used to develop a thermodynamic and physical black-oil model capable of simulating the behavior of the reservoir fluids under the various operating conditions. Little information is available to estimate the physical properties of the reservoir fluids. The properties known include an oil API gravity of 40° (Lytle, 1950), and bubble point pressure of 780 psia (Pennzoil, 1985).

There is no information about the composition or properties of the gas present in the Taylorstown reservoir. The specific gravity of this gas was determined to be 0.9 using a gas chromatographic analysis. Gas Analysis Systems Inc performed this analysis, in June 2001. The water specific gravity was assumed constant and equal to 1.0, and the gas phase was assumed immiscible in the water phase. Also, it was assumed that the temperature of the reservoir remains constant at all times.

Given the sparse information known about the properties of the fluids present in this field, a PVT model was developed using published correlations. The PVT model developed is a black-oil model, with the capability to simulate dissolved gas in the oil phase.

The PVT model requires the determination of certain properties at different pressure conditions. For the oil phase, these properties were: solution gas-oil ratio (R_s), oil formation volume factor (B_o), oil compressibility (c_o), and oil viscosity (μ_o).

The solution gas-oil ratio at different pressures was estimated using a correlation developed by Glaso in 1980. This correlation is shown below:

$$R_s = \gamma_g \left[\frac{API^{0.989}}{T^{0.172}} 10^{Y} \right]^{1.22549}$$

where:

R_s = solution gas-oil ratio, SCF/STB_O

T = temperature,°F

API = oil API gravity

γ_g = specific gravity of the gas at standard conditions

and Y is defined as follows:

$$Y = \frac{1.7447 - \sqrt{5.1797 - 1.2087 * \log(p)}}{0.6044}$$

where:

p = pressure, psia.

The oil formation volume factor was determined using the following correlation developed by Standing:

$$B_o = 0.972 + 0.000147 F^{1.175}$$

where:

B_o = oil formation volume factor, bbl/STB_O

The F factor is determined using the following equation:

$$F = R_s \sqrt{\frac{\gamma_g}{\gamma_o}} + 1.25T$$

where:

R_s = solution gas-oil ratio, SCF/STB_O

T = temperature,°F

γ_g = specific gravity of the gas at standard conditions

γ_o = specific gravity of the oil at standard conditions

The oil compressibility was determined by means of the Vazquez and Beggs correlation shown below:

$$c_o = \frac{(1433 + 5R_s + 17.2T - 1180\gamma_{gc} + 12.61API)}{10^5 p}$$

where:

c_o = oil compressibility, psi^{-1}

R_s = solution gas-oil ratio, SCF/STB_O

T = temperature,°F

API = oil API gravity

γ_g = specific gravity of the gas at standard conditions

γ_o = specific gravity of the oil at standard conditions

p = pressure, psia

Finally, the oil viscosity was estimated using the Beggs & Robinson correlation. The viscosity of the live oil is determined by:

$$\mu_{ol} = \left(10.715(R_s + 100)^{-0.515}\right)\mu_{od}^{\ b}$$

where:

μ_{ol} = viscosity of the live oil, cp

μ_{od} = viscosity of the dead oil, cp

R_s = solution gas-oil ratio, SCF/STB_O

The *b* factor is calculated by the following equation:

$$b = 5.44(R_s + 150)^{-0.338}$$

The viscosity of the dead oil is estimated using the correlation shown below:

$$\mu_{od} = 10^x - 1$$

where x is calculated as:

$$x = \frac{10^{(3.0324 - 0.02023 API)}}{T^{1.163}}$$

For the water phase the only properties estimated at different pressures were the water formation volume factor (B_w), the water compressibility (C_w), and the water viscosity (μ_w). The water formation volume factor was estimated by means of the Gould correlation:

$$B_w = 1.0 + 1.2x10^{-4}(T - 60) + 1.0x10^{-6}(T - 60)^2 - 3.33x10^{-6} p$$

where:

B_w = Water formation volume factor, bbl/STB_W

T = temperature,°F

p = pressure, psia

The water compressibility was calculated using the Meehan correlation for gas free water.

$$c_w = 10^{-6}\left[A + BT + CT^2\right.$$

where:

c_w = water compressibility, psi^{-1}

T = temperature,°F

and the variables A, B, and C are defined as:

$$A = 3.8546 - 0.000134p$$
$$B = -0.01052 + 4.77x10^{-7} p$$
$$C = 3.9267x10^{-5} - 8.8x10^{-10} p$$

where:

p = pressure, psia

The water viscosity is estimated by means of the Beggs & Brill correlation, shown below:

$$\mu_w = \exp\left(1.003 - 1.479x10^{-2} T + 1.982x10^{-5} T^2\right)$$

where:

μ_w = water viscosity, cp

T = temperature,°F

For the gas phase, there was the need to determine the gas compressibility (B_g), and the gas viscosity (μ_g) at various pressures. The formation volume factor was determined using the real gas equation of state, where:

$$B_g = 0.0283\frac{ZT}{p}$$

where:

B_g = gas formation volume factor, Cf/SCF

T = temperature,°R

p = pressure, psia

z = gas compressibility factor

To calculate the viscosity of the gases, the Lee et al. correlation (1966) was employed. This correlation is shown below:

$$\mu_g = K \times 10^{-4} \exp\left[X\left(0.0433\rho_g \frac{p}{Z(T+460)}\right)^Y\right]$$

where:

μ_g = gas viscosity, cp

T = temperature,°R

p = pressure, psia

z = gas compressibility factor

The variables K, X and Y are defined as follows:

$$K = \frac{(9.4 + 0.02M_a)(T+460)^{1.5}}{209 + 19M_a + (T+460)}$$

$$X = 3.5 + \frac{986}{(T+460)} + 0.01M_a$$

$$y = 2.4 - 0.2X$$

where:

M_a = Molecular weight of the gas.

Even though the fluid properties available to build the model were sparse, the correlations and assumptions employed allowed building a complete PVT model that is able to simulate the behavior of the three phases involved in the reservoir.

2.3 Rock properties

The rock properties needed to perform this simulation study are: porosity, initial saturations, absolute permeability, relative permeability, and capillary pressures characteristics. The porosity in different locations of the field was determined using pore-feet maps provided by the operator of the field. This pore-feet map allowed estimating the porosity in the center of all the grid blocks of the field. The porosity values discretized ranged from 16% to 35%.

A gas saturation map was provided, and it was used to define the initial gas saturation of each grid block at the beginning of the waterflood operations. The only information available to estimate the water saturation of this field was 12 resistivity logs, which were obtained from the 12 injection wells. These logs showed that the water saturation in the injection wells ranged from 12% to 32%, with an average of 20%. The location of the measurements of water saturation did not allow interpolating the saturation values towards the boundaries of the field; therefore, a value of water saturation of 20% was initially assumed for the entire reservoir.

There was one core analysis available for use in the Taylorstown study: Core laboratories performed the analysis on a core obtained from the John Mc Mannis 1 Well. The information provided in this core analysis was used to feed the simulator with an estimate of the absolute permeability, relative permeability (Figure 2.6), and capillary pressure for this sandstone (Figure 2.7).

The arithmetic average absolute permeability that was determined using the core analysis is 100-md. Since this core analysis was the only one available for the field, the absolute permeability obtained was used to initialize all blocks in the simulator.

The relative permeability curves obtained from the core analysis (Figure 2.6) show that for values of water saturation below 30%, the relative permeability of the displacing phase (water) has values below 0.001. The low relative permeability of the water suggests that the mobility of the displacing phase is small. Given this, the model was unable to simulate the water injected in the field.

Several preliminary runs were made to determine if relative permeability values obtained from the core analysis are representative of the field wide permeabilities. Results indicated that a satisfactory match of field behavior was not attainable. Given this, another approach was necessary. The relative permeabilities curves obtained from the analysis of a core taken from the L.S. Hoyt 100 well (LSH 100) in the Wileyville field were tested for applicability (Figure 2.7) The justifications for this approach are that both the Taylorstown and Wileyville fields are geographically near one another, and produce from the same reservoir, the Gordon Sandstone.

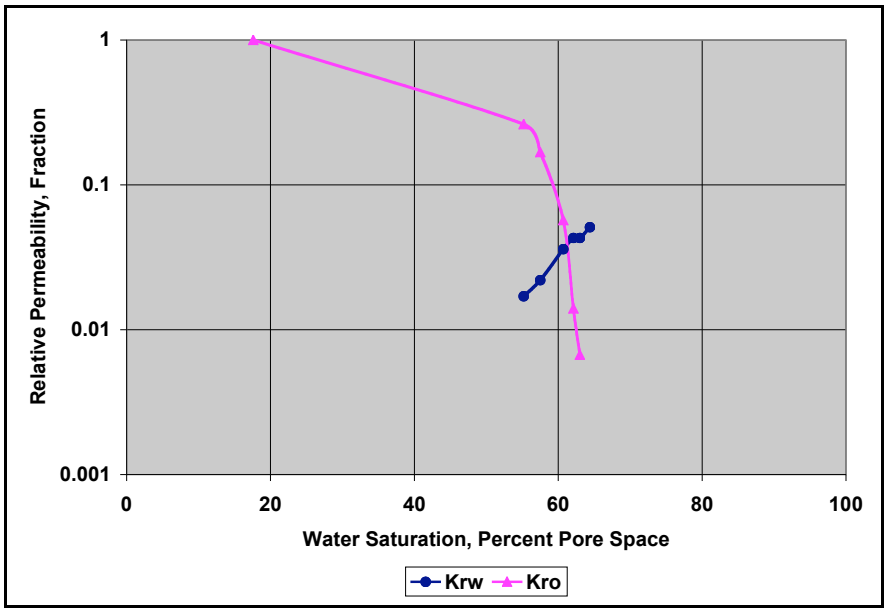

Figure 2.6. K_r vs. Sw (John McMannis 1 Well, Taylorstown Field)

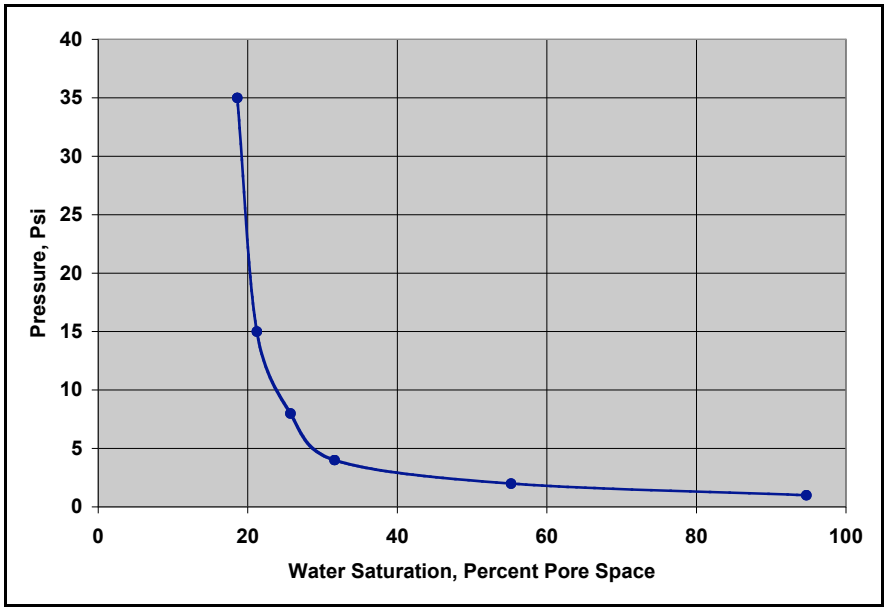

Figure 2.7. Capillary pressure vs. S_w. (James McMannis 1 Well, Taylorstown Field)

3.0 RESULTS AND DISCUSSION

After the initialization of the data, the model is run to determine the similarity between the trend and value of the results of the simulation and the data obtained from the field. The results of this first run indicate the regions of the reservoir where the assumptions made can be considered to be a "good" approximation, and give the modeler a hint about the properties that must be adjusted in order to make the simulation match the behavior of the field. It is the good initialization of the reservoir properties along with a clear description of the history of each field that allows an efficient history matching process and the best representation of the actual behavior of the reservoir.

Given the sparsity of the data available for the construction of the models of this study, several assumptions and correlations were made. The most critical assumptions are:

1. These reservoirs could be modeled as two-dimensional single layered models with uniform properties throughout the thickness of the sand,
2. Extrapolation of fluid and rock properties from studies made in other fields within the same basin where the Gordon sandstone is undergoing waterflooding,
3. Application of a black-oil model based on published correlations using only the specific gravity of the oil and gas present in this field.

The guidelines for history matching are applied to the Washington-Taylorstown field. This section of the chapter discusses the results obtained from the initialization of the parameters, the results of the history matching, and the results of the predictive phase of the study for the Washington-Taylorstown field.

3.1 Results of the initialized model

Figure 3.1 compares the results of the actual and simulated field water injection rates for the first run following the initialization of the study. As the plots indicate, the shapes of the simulated and the actual curves are similar. This similarity validates the general trend in the behavior of water injection in the model. In addition, Figure 3.1 shows that the water injection decline is at a higher rate than that expected if

uniform permeability is assumed throughout the reservoir. The abrupt changes in injection rate coincide with the dates when workovers were undertaken. These changes reflect the positive impact on the injectivity of the field of individual well workovers.

Figure 3.2 compares trends of the simulated cumulative production after the initialization of the model to the actual production observed in the field. It shows that the trend of the simulated curves is similar to the trend of the cumulative production observed in the field. This validates the ability of the model to recreate the production trend of the field. The results observed for each well permitted the identification of the regions of the model where the permeabilities and or the saturations need to be adjusted to make the model match the actual behavior of the field. The results of this run revealed that for most wells the cumulative liquid production has a similar behavior, even though the cumulative production of each phase does not approximate the value expected.

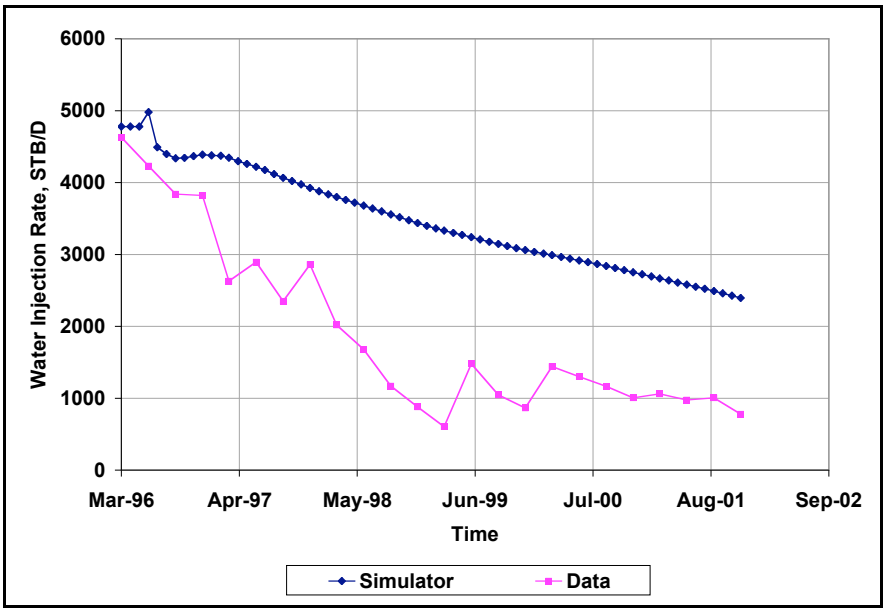

Figure 3.1. Field water injection rate vs. time. Field data vs. simulation results.

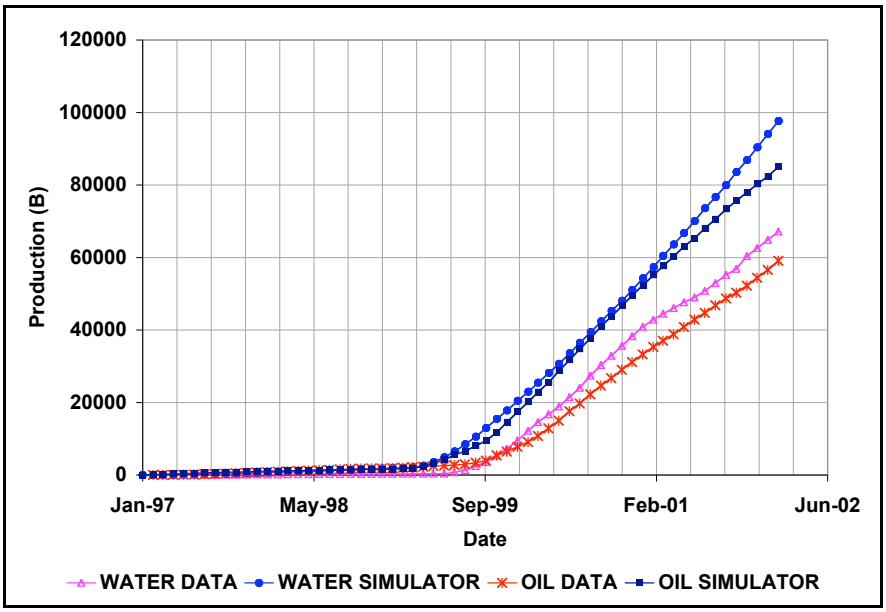

Figure 3.2. Field cumulative production vs. time. Field data vs. simulation results

Even though the results of the individual wells do not match the behavior shown in the field in terms of oil and water cumulative production, initialization of the model using the sparse information available has proven to be an acceptable starting point for the history matching. As indicated earlier, this initial approximation provides the basis for identifying the parameters that need to be changed and their field location.

3.2 History matching results

After several iterations during which the "unknown" parameters in the model were adjusted, a satisfactory history match was achieved. The results show an acceptable behavior of the model, which mimics the operations of the field since the beginning of the waterflooding, during February of 1982, to the end during January of 2002. The results of the history matching are analyzed in this section.

3.2.1 Discussion of the results of the injection match

The comparison of the actual and the simulated water injection rates confirm that the trends of both curves are qualitatively similar for all injection wells. Figure 3.3 shows that the simulated water injection

rate curves are similar in shape and trend to the actual water injection curve for every well. In addition, it can be seen that the simulated water injection rate on a field scale is in good agreement with the actual water injection curve of the field.

The second step in the analysis of the results is to compare the actual and the simulated water injected volumes for each well. These volumes are computed for the actual operation and for the simulation, and the results compared. Figure 3.4 shows the difference between the actual and the simulated water volumes for each injection well. The relative error in the water-injected volumes is calculated for every well and the results reported in Figure 35. In this figure it can be seen that the error in 11 of the 12 injection wells is below 18%, which is considered to be "acceptable" for this study.

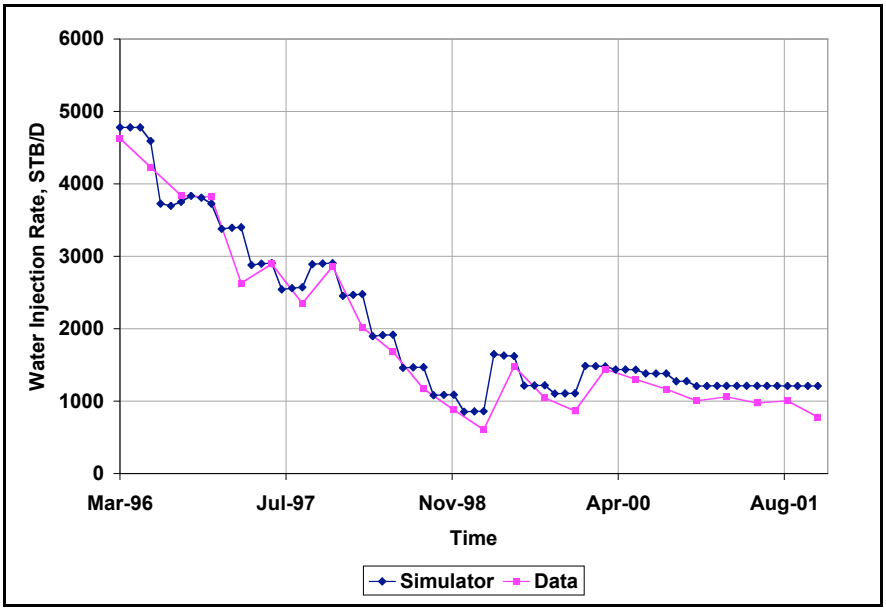

Figure 3-3. Field water injection rate vs. time. Field data vs. simulation results

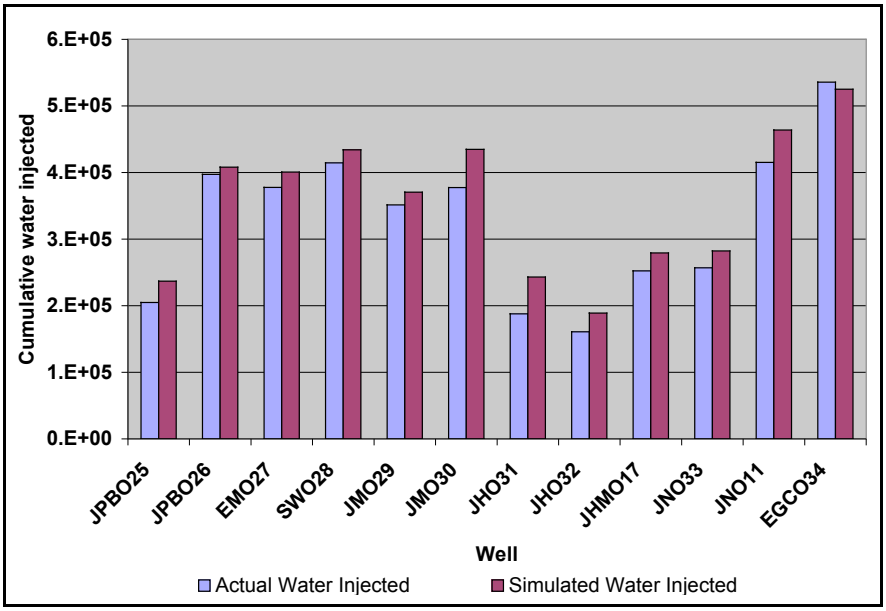

Figure 3.4. Comparison of the water injected volumes. Field data vs. simulation results

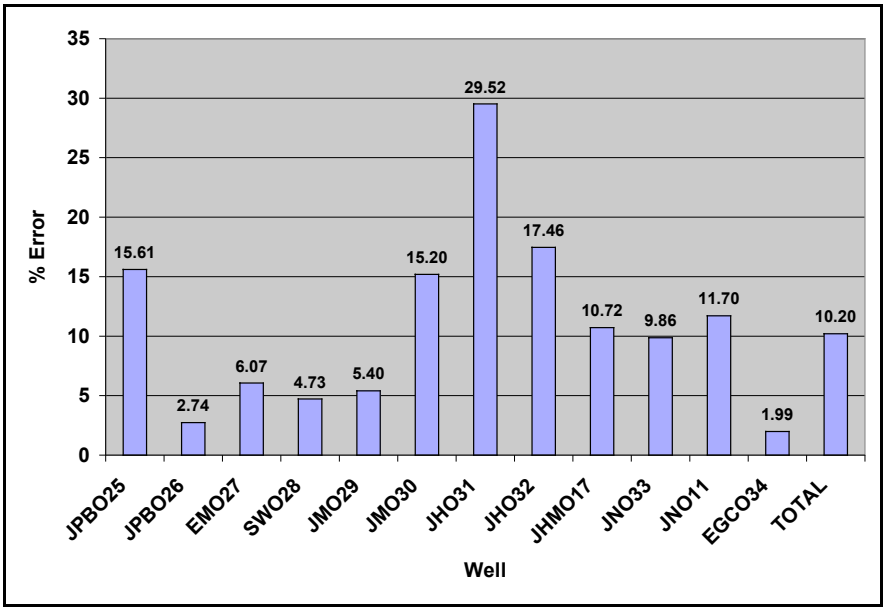

Figure 3.5. Relative error computed for the water volumes injected

The James Hodgens 031 (JHSR 031) well is the only well where the error is greater than 18%. However, the absolute difference between actual and the simulated water volumes injected by this well is small (about 55,000 barrels). When compared to the volume injected in the field, this represents only about

2% of the total water volume injected; therefore this error is considered to be not significant. The total water injection of the field is within a 10% error, which is considered to be an acceptable match for this study.

3.2.2 Discussion of the results of the pressure match

Table 3.1 shows that all the pressures calculated by the model match the pressures obtained from the field, within an error margin of 20%. As previously noted, fluid levels were calculated using an acoustic device. The error associated with this measurement include imprecise fluid height and lack of knowledge of column density. As a consequence, an error of 20% was determined to be reasonable.

Only two pressures calculated in the simulation are not within this margin of error. These pressure readings correspond to Samuel Woodburn 11 (SW 11) and James Paul Bigham 4 (JPB 4) wells. The behavior of these wells shows an abrupt decline in the fluid level readings and liquids production. It was concluded that the wellbores of these wells might be damaged and the skin factor of such magnitude suggested that there was no communication with the reservoir sand. Therefore, the measured data were considered to be unrepresentative of the pressure conditions present in the reservoir.

Even though the error computed for the James Hodgens Sr. 10 (JHSR 10) and J. A. Flack 3 (JAF 3) wells is greater than the margin of error, the absolute difference in the pressure values is not significant (about 60 psi), and this difference might be attributed to the resolution of the instruments used to read the fluid levels in the field.

WELL	LOCATION	DATE	REAL	SIMULATED	ERROR (%)	COMMENTS
JH1	9,32	Dec-99	386	340	11.92	
JN2	9,30	Dec-99	500	472	5.60	
JPB4	7,9	Dec-99	92	183	98.91	BLOCKED
SW11	6,15	Dec-99	37	132	256.76	POSSIBLY BLOCKED
EM1	10,12	Dec-99	190	201	5.79	
JN3	7,29	Dec-99	400	447	11.75	
JHSR9	8,36	Oct-01	256	243	5.08	
JHSR10	10,38	Oct-01	276	202	26.81	
JAF3	9,39	Oct-01	240	187	22.08	

Table 3.1. Actual pressures measured vs. Pressures simulated

3.2.3 Discussion of the results of the production match

Figure 3.6 compares the actual and the simulated cumulative production of oil and water respectively. The trends of the actual and the simulated curves are similar in both shape and value, giving a good qualitative match. The simulated and the actual oil and water production of each well is also similar in both shape and value, resulting in a good match.

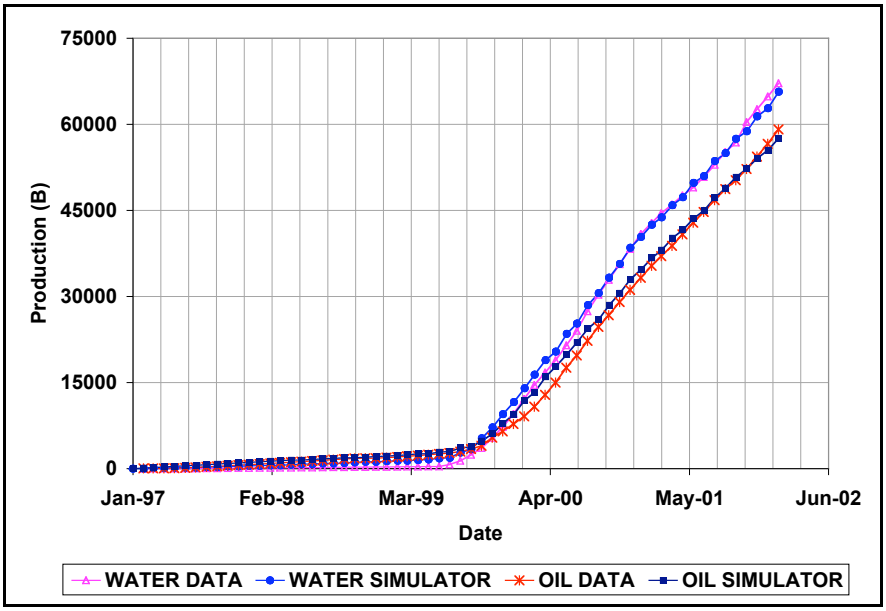

Figure 3.6. Oil and water production of the field vs. time. (Field data vs. sim. results)

Figure 3.7 indicates that the error in the match for the cumulative oil production for each well is less than 10% for most of the wells. In addition, in those wells where the error is greater than 10%, the difference in the oil production is not significant when compared to the total oil production of the field (Figure 3.8). The error in the most prolific wells (J. A. Flack 1 (JAF 1), and V.M. Blayney 22) is less than 10%.

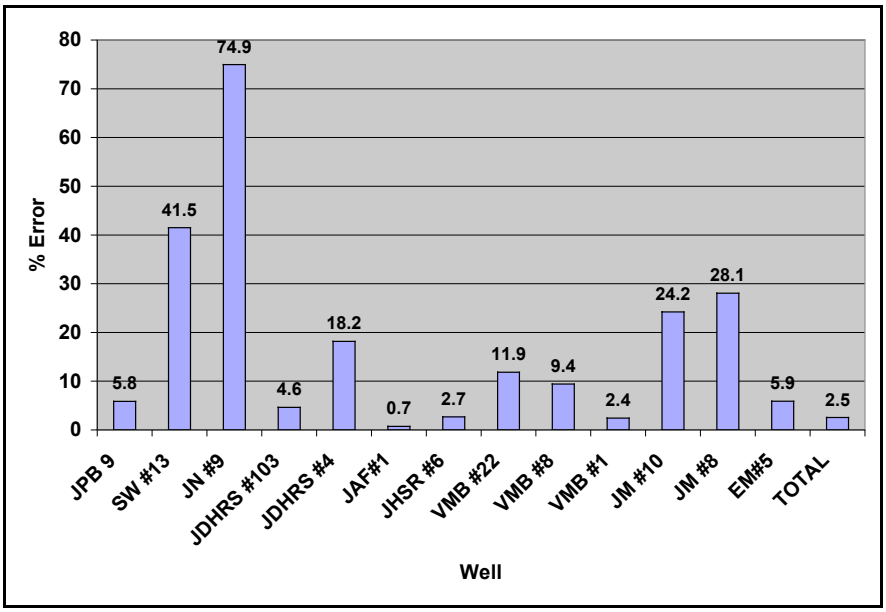

Figure 3.7. Error in the cumulative oil production per well

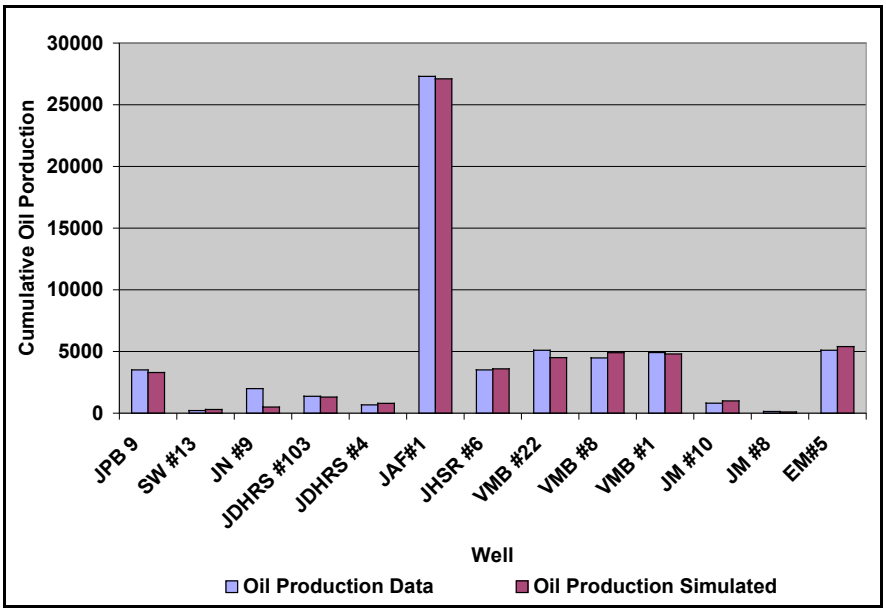

Figure 3.8. Comparison of oil production per well (February 2002)

The deviation in the oil production is less than 10% for 8 of the 13 wells, in three wells (JDHRS 4, JM 10, and JM 8) the disparity was slightly higher than 10% (around 20 %), and the only wells showing a significant disparity are wells James Noble 9 (JN 9) and Samuel Woodburn 13 (SW 13). In any case, the production of these wells is small and it is not significant when compared to the production rates of other

wells in the field. Figure 3.8 compares the actual and simulated cumulative oil production per well. The results show good agreement between the predicted and observed values for each well. In addition, it shows that even though the error is greater than the "acceptable" for wells JN 9, SW 13, JDHRS 4, JM 10, AND JM 8, the difference between the volumes produced and predicted through simulation is small in terms of absolute production. For these wells, the differences in the volumes actually produced and simulated are explained by the fact that production is intermittent. As a consequence, the actual production does not have the "exact" production schedule as that predicted through simulation.

The error in the predicted water production is less than 10% for 10 of the 13 wells (Figure 3.9). This is considered to be an acceptable error, given the fact that the actual production and the simulated production did not have the same production profile. Figure 3.10 is used to compare the actual and the simulated cumulative water production per well. Figure 3.10 shows that the actual cumulative water produced is similar to the predicted from simulation for each well. In addition, it shows that even though the error is greater than "acceptable" for wells JPB 9, and EM 5, the difference between the volumes produced and simulated is small when compared to the total water production. For these wells the difference in the volumes actually produced and that predicted through simulation is explained by the fact that production is intermittent, and consequently actual production schedule is not an exact replication of the production schedule used in the simulation.

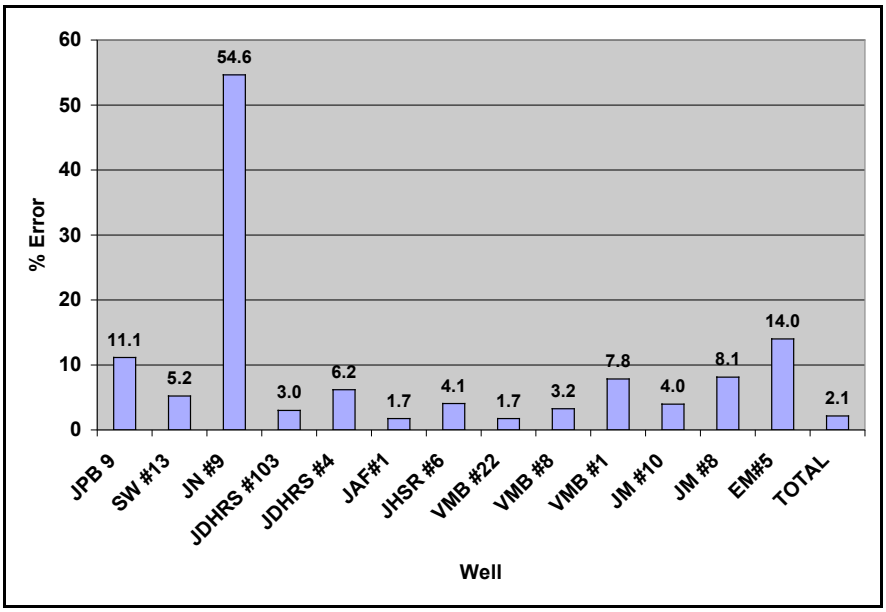

Figure 3.9. Error in the cumulative water production per well

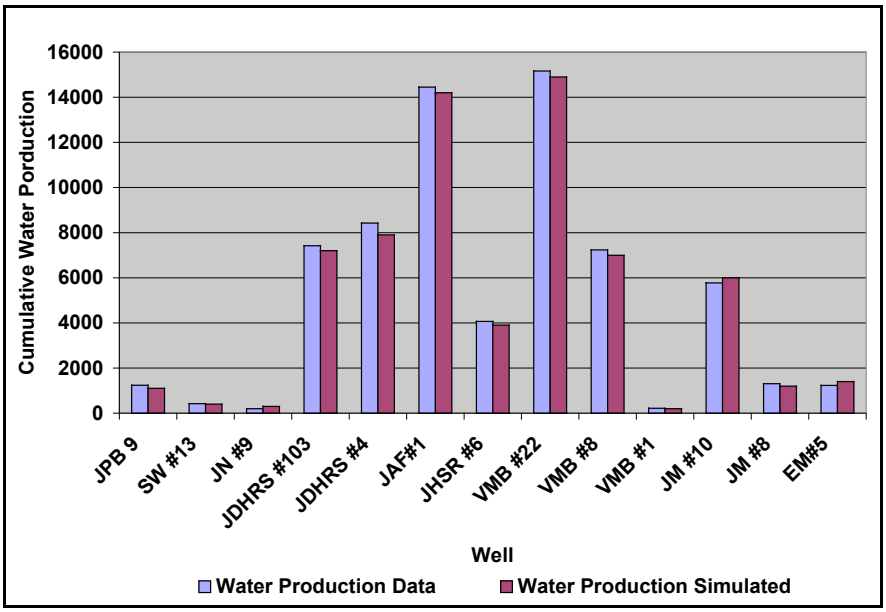

Figure 3.10. Comparison of water production per well (February 2002)

Only one well shows a significant error in the cumulative water produced, James Noble 9 (JN 9) well. This well shows a deviation because it underwent a workover on November 2001, and the data indicate a sudden increase in oil and water production. The trend during recent months is not of sufficiently long duration for matching to be attempted for this well. Nevertheless, the simulation could not match the

sudden increase in additional oil production. This was because the workover of this well resulted in a significant decrease in the near wellbore damage and the model could not approximate this behavior. This increase in production amounted to 1,500 barrels that represents only about 2% of the total oil volume produced. This is not significant when compared to the total oil production of the field.

When the history match is considered to be acceptable, the results of the simulation are representative of the past and present behavior of the reservoir. Observations were then made about the impact of the multiple sources of water on the injection and the influence of the water injected during the injection pilot on the current production of the field.

3.3 Discussion on skin damage

Skin is a mathematical representation of formation damage or stimulation and represents a decrease or increase in apparent permeability. Physically, damage can result for a variety of reasons such as clay swelling and/or fines migration. In the case of fluid injection as in secondary recovery, the cause of this damage may be the precipitation of unfiltered solids or injected fluids-formation incompatibility. Dynamic skin reflects the variation of this formation damage with time and represents the physical reality of well operations over time.

In this study, the analysis of the dynamic skin is undertaken in the context of waterflooding and it is determined during the history matching process through inference. This is accomplished by varying the values of S, skin factor, to match well and field performance. To analyze the change in S with time, plots needed to be constructed and analyzed.

The case study involves the Washington-Taylorstown field. The analysis is carried out in two steps. First the dynamic behavior of the skin in the injection wells, where this effect is more pronounced, is initially addressed. The phenomenon is then extended to the production wells. Since the movement of the fluids starts in the injection wells and moves toward the production wells, analysis of the skin factor in the two types of wells will provide quantitative information on the time dependency of skin damage.

To accomplish this analysis, the Washington-Taylorstown field was subdivided into regions. The criteria employed in the classification of the different regions were: 1) the type of well, either injection or production, 2) the physical location of the well and, 3) the similarity in the dynamic skin behavior in the well. Figure 3.11 shows the regions for the case study. Historical injection and production rates were constructed and analyzed for each region. The results obtained are discussed below.

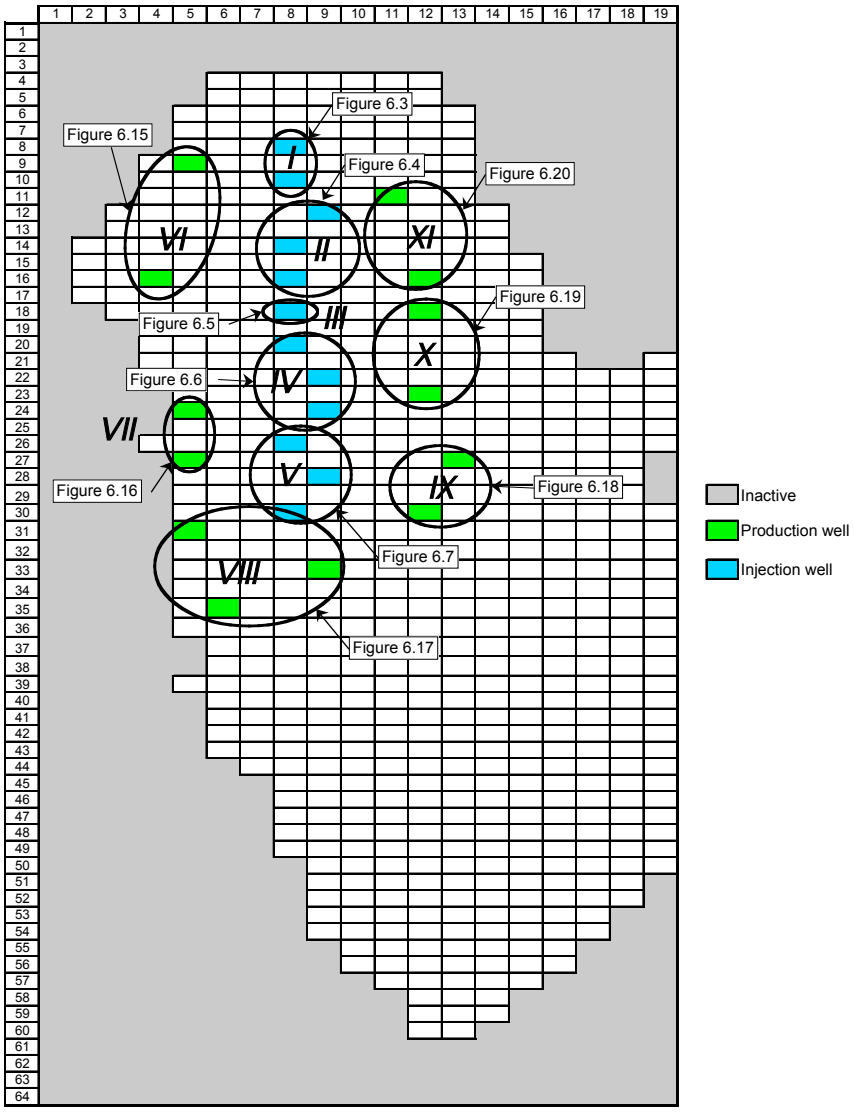

Figure 3.11 Washington-Taylorstown field regions.

As indicated earlier, the Washington-Taylorstown field has been subjected to waterflooding since February 1982, when an injection pilot located in the southern portion of the field was developed. Based on the results of this pilot project, it was concluded that this reservoir had potential for waterflooding. This conclusion was based on the fact that suitable injection rates were achieved and production responses were noted in nearby wells. Based on the results of the pilot, field scale flooding was undertaken.

3.3.1 Discussion of the results on skin damage in injection wells

Field scale waterflooding using a line-drive pattern began in March 1996. From March 1996 until March 1999, the water used for the injection was obtained from an abandoned coalmine and/or produced brine from gas fields operated in the area. One potential problem with the use of water from unconventional sources of water is the potential for reservoir damage attendant to the transport of the unfiltered solids into its matrix. Added to this is the fact that incompatibility of the formation fluids with the injection fluid can potentially create chemical reactions in the matrix. Chemically treated freshwater injection began in March 1999, and has continued to the present.

As the plot indicates (Figure 3.12), the injection history is broken into two periods. During Period I, the source of the water injected was from an abandoned coalmine and brine from a gas producing formation. This practice ended in March 1999. During Period II, the source of injected water was from a municipal water system. As previously indicated, this water was treated with a chemical to minimize its impact on the formation.

During the first injection period, the injectivity of the field declined from 4.6 Mbbl/d to 600 bbl/d. It is noted that during this period, efforts were made to improve the water injection rates. The loss in injectivity is attributed to the following factors:

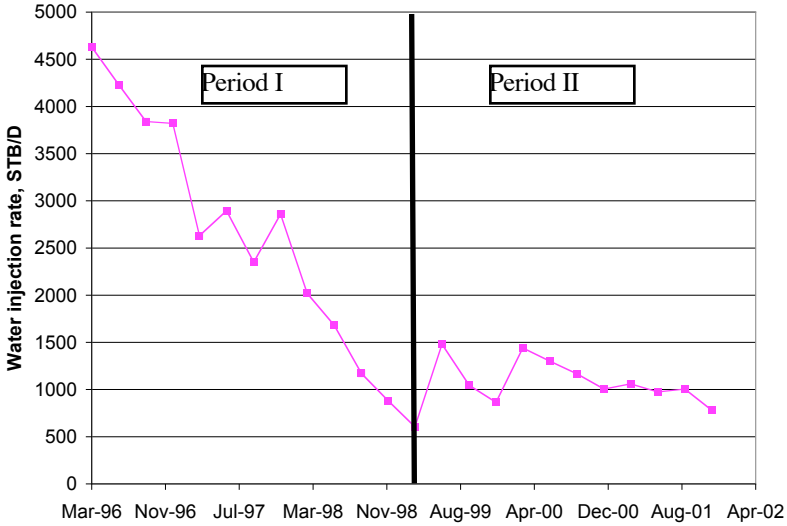

Figure 3.12: Washington-Taylorstown field, periods of water injection.

1) Natural fill up that is attendant to liquid injection.
2) Fill up resulting from the introduction of unfiltered solids.
3) Fill up resulting from the formation of a viscous sludge, i.e. emulsions.
4) Blockage of pore space throats that reduces the formations absolute permeability near the wellbore.

The erratic behavior of the injection rate with time suggested wellbore skin problems. Consultation with the operator, however, indicated that efforts were made to alter this behavior by well workovers, stimulations and chemical treatments. As the results on Figure 3.12 indicate, the effects of these treatments were short-lived.

To better understand the injectivity problem, the Washington-Taylorstown field was divided into eleven regions. Five of the eleven regions contain the 12-injection wells and the other six the 23-production wells. The locations of the eleven regions are shown on Figure 3.11. Figures 3.13 to 3.17 contain plots of the skin damage versus time and the water injection rate for each of the injection wells found in regions I though V. Each of the figures indicates a decrease in injection rate with time. The operator's effort to

reverse this decline in injectivity through acidizing resulted in a short-lived increase in injectivity followed by a decrease.

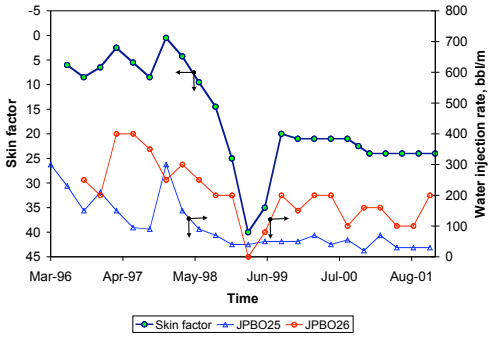

Figure 3.13: Skin factor in injection wells JPBO25 and JPBO26 of Washington-Taylorstown field.

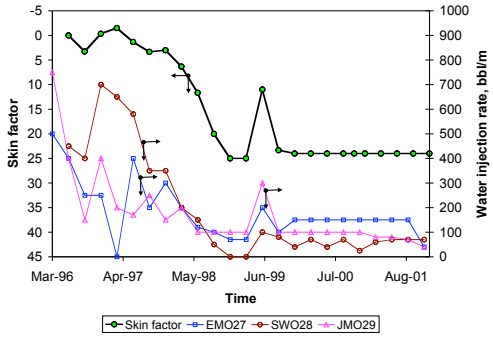

Figure 3.14: Skin factor in injection wells EMO27, SWO28 and JMO29 of Washington-Taylorstown field.

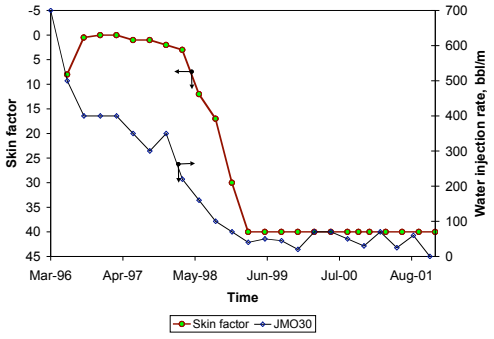

Figure 3.15: Skin factor in injection well JMO30 of Washington-Taylorstown field.

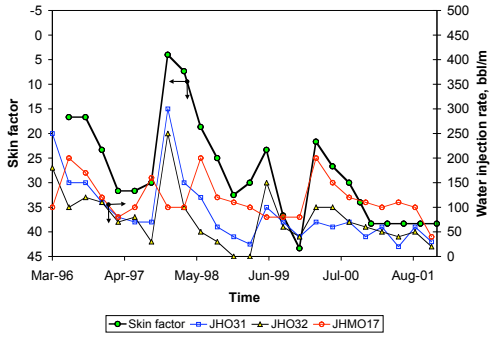

Figure 3.16: Skin factor in injection wells JHO31, JHO32and JHMO17 of Washington-Taylorstown field.

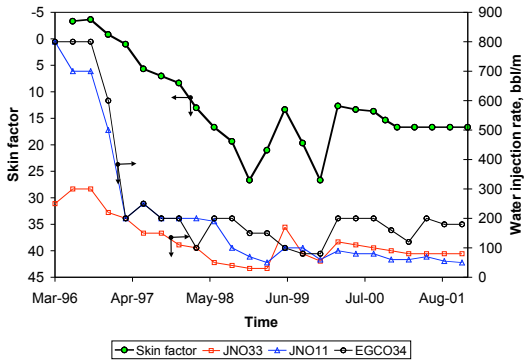

Figure3.17: Skin factor in injection wells JNO33, JNO11 and EGCO34 of Washington-Taylorstown field.

This cycle of well stimulation followed by a decline in injection rates was repeated until the start of fresh water injection (by mid 1999 and early 2000). Even though injection rate continues to decline with the switch to fresh water, the rate of decrease is smaller (see Figure 3.12). During Period II, it should be noted that the operator undertook a series of workovers and acidizing jobs. This combined with the use of treated water resulted in a field-wide increase in injectivity. The field injection rate had dropped to 600 bbl/d prior at the start of fresh water injection. The injection rate increased to 1.4 Mbbl/d. However after 6 months, the injectivity decreased again to 860 bbl/d. After acidizing the wells of higher injectivity, the field injection rate again increased up to 1.4 Mbbl/d. Since then, a general and steady decline in the injection rate has been reported reaching today's value of approximately 700 bb/d.

The skin factor coincidental to the use of treated fresh water has stabilized (see Figures 3.13 to 3.17). Efforts to decrease the skin were unsuccessful because the damage resulting from the use of unconventional water (coal mine – brine) and air flooding was spread throughout the reservoir. What is envisaged with respect to this process is shown on Figure 3.18. The concept suggested is one where stimulation of each well penetrates further and further from the wellbore; but the damaged zone is so pronounced that its effect on injection rate is soon felt.

In addition to the change of water source there are other variables to consider that may affect the skin. At the beginning of the 20th century, this field was subjected to gas-air flood stimulation. With the presence of oxygen in the reservoir, chemical reactions may take place leading to the production of

emulsion, which may promote blockage of the reservoir. Besides, the oxidation of the metallic elements in the injection wells is expected to precipitate ferric compounds, which may also be deposited in the reservoir.

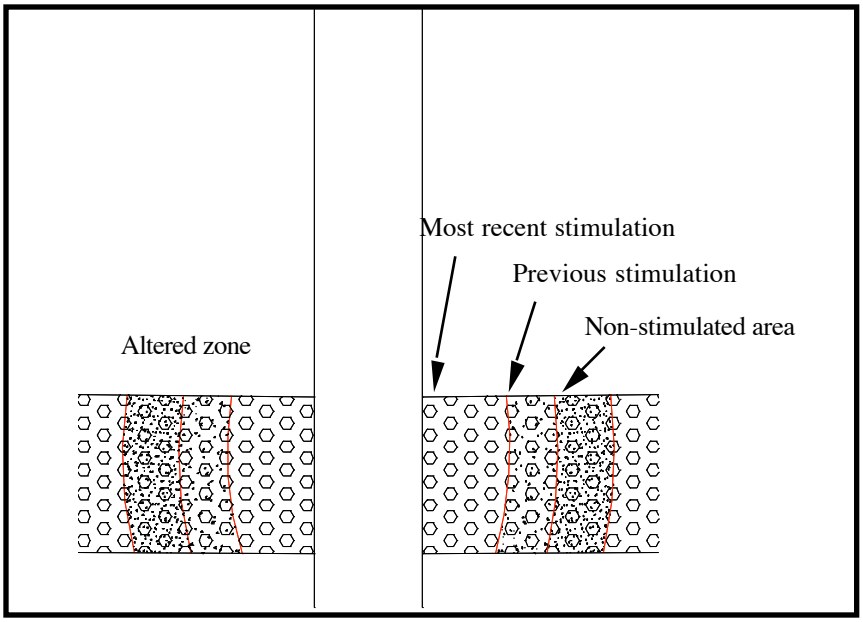

Figure 3.18: Formation skin damage after cyclic stimulations.

For Period II, 1999 to today, each of the injection wells possesses a similar performance as it is described at the field scale. Wells JPBO25 and JPBO26 (Figure 3.13) and wells EMO27, SWO28 and JMO29 (Figure 3.14) show reduced skin damage that coincides with acidizing and the use of treated fresh water for injection. It should be noted that two stimulation jobs were performed after the initiation of fresh water injection. The first was after 3 months and the second after 9 months. In both cases, the skin damage was reduced, but with time increased and stabilized at values of approximately 25. As was expected, injectivity behaved in an opposite manner. The trend following stimulation indicated an increase followed by a decrease and then stabilization at a lower value.

Wells JHO31, JHO32 and JHMO17 (Figure 3.16) and wells JNO33, JNO11 and EGCO34 (Figure 3.17) showed a better response to the change of the injected water. The impact of skin factor showed

improvement through reduction immediately following the stimulation jobs. However after 3 to 4 months, skin damage increase was evident as reflected in the decrease in injection rates.

The behavior of well JMO30 (Figure 3.15) is unusual when compared to other injection wells in the field. The change of injected water did not affect the behavior of the well, even though stimulation jobs have been performed. This response is attributed to the location of the well in the region with poor properties that separates the northern and southern portions of the field. Although treated water is now being injected, the effect of the deposited particles from the untreated water continues to be felt. It is thought that the injection rate will steadily drop even with additional stimulation.

3.3.2 Discussion of the results on skin damage in production wells

Production well behavior as would be expected is different than injection well behavior. This is because liquid production is dependent on the location of the flood front as it moves throughout the reservoir and the saturation distribution present in the vicinity of the production well. Each well behaves in a unique fashion and as a consequence, no generalization concerning production behavior can be made. In this field, wells J.A. Flack 1, V.M. Blayney 1, V.M. Blayney 8, V.M. Blayney 22 and J.P. Bigham 9, are the principal liquid producers. Other production wells in the northern and western portions of the field produce little or no liquid. In the case of the wells located in the northern section, the presence of the high gas saturation precludes liquid production and in the case of the wells located in the west, the flood front has not yet arrived. The focus of this analysis in terms of skin is the liquid producing wells or those where liquid production can be realized through workovers.

The production of oil and water at the field level increased in late 1999. This increase in production was coincidental to the start of treated fresh water injection. This observation is based on the presupposition that fill up of the reservoir was mainly completed and that displacement of both reservoir oil and formation water had reached several of the production wells. In wells SW13, JDHRS103, JDHRS4, JHSR6, JM10, JM8 and EM5, breakthrough had occurred with a resulting production of mostly water. In wells JAF1,

wells JAF1, VMB1 VMB8, VMB22 and JPB9 breakthrough has not occurred and as a consequence, production of both oil and water are realized.

Figure 3.19 shows the water saturation as of March 2002. The figure indicates that wells JN9, JDHRS4 are located in areas of high water saturation and as expected produce mostly water. Wells JAF1 and JPB9 are located in areas where the oil saturation is high and produce both oil and water.

As previously indicated, the injected water is displacing particles in suspension toward the production wells. As a consequence the production of the wells is being affected by the particle displacement. The analysis indicates that skin resulting from the displacement increases prior to the onset of displaced water. Prior to the arrival of these displaced liquids, the skin damage was in the range of 0 to 5. With breakthrough, these values increased to a range between 40 and 50. It should be noted that this effect is long lasting and the efforts to reverse it through reconditioning of the wellbore result in only short lived increases in productivity (approximately 3 months) and that the production then begins to experience a pronounced decline.

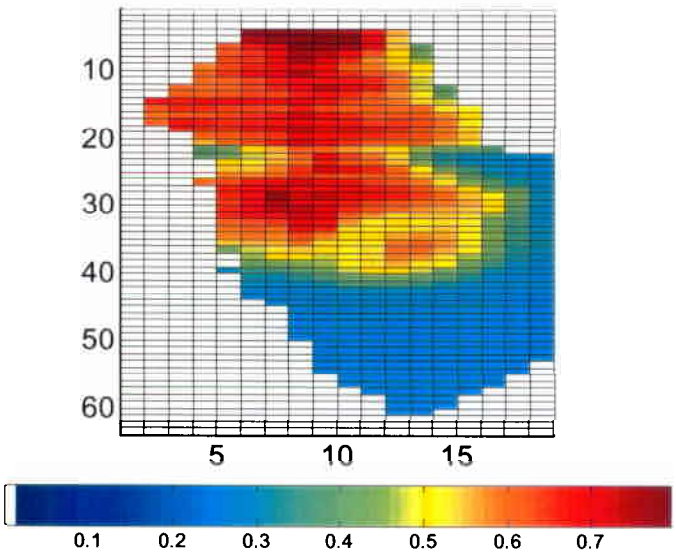

Figure 3.19: Washington-Taylorstown field, water saturation map by March 2002.

This performance is illustrated in wells JPB9 and SW13 (Figure 3.20). This figure indicates that skin damage increased dramatically during the second half of 2000. Liquid production also declined from 400 bbl/m and 25 bbl/m to almost no production in wells JPB9 and SW13, respectively. In January of 2002, workovers reversed this decline in productivity and reduced skin from 50 to 20. Examination of Figure 6.10 indicates that this performance can be attributed to the arrival of the flood front and the presence of suspended particles in the flood front that damage the reservoir.

Similarly, the performance of the wells JN9 and JHRS103 (Figure 3.21) has been impacted by the displacement process. Stimulation resulted in an improved performance. But, after only 3 months productivity began to decrease.

As indicated in Figure 3.22 and Figure 3.23, the impact of the displacement in terms of the arrival of flood front has not occurred. These wells have no significant skin damage and are producing significant amounts of liquid. It is expected however, given the performance of wells JDHSR6 and JAF1 (Figure 3.22) and wells VMB8 and VMB22 (Figure 3.23), that with the arrival of the flood front, skin damage will increase and well productivity will decrease.

In the case of wells VMB1 and JM10 (Figure 3.24) and wells JM8 and EM5 (Figure 3.25) the flood front has only begun to impact the performance. This is illustrated in Figures 3.24 and 3.25 where skin damage has increased and productivity decreased.

In summary, the injection of the water from coalmines and gas field brine has significantly affected the productivity of the field. The time dependant variation in the skin damage is estimated from the decline in the productivity of the wells located in the field. The results of these analyses will permit the operators of the field to perform efficiently schedule well workovers and stimulations.

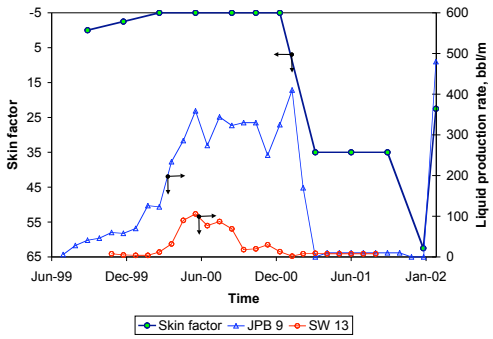

Figure 3.20: Dynamic skin in production wells JPB9 and SW13 of Washington-Taylorstown field

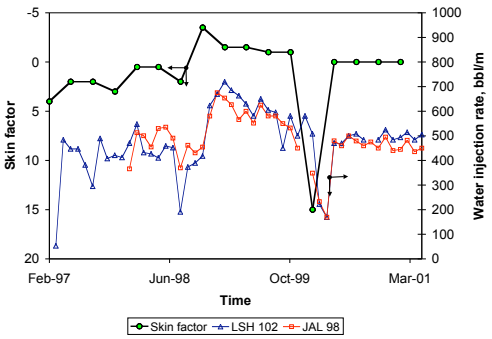

Figure 3.21: Dynamic skin in production wells JN9 and JDHRS103 of Washington-Taylorstown field

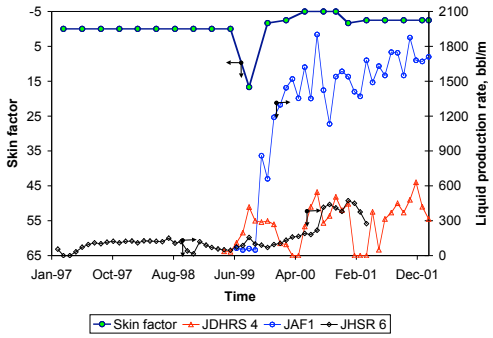

Figure 3.22: Dynamic skin in production wells JDHRS4, JAF1 and JHSR6 of Washington-Taylorstown field

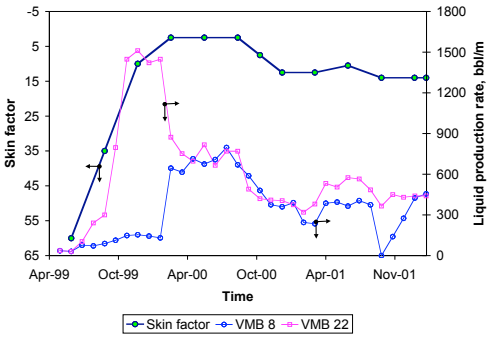

Figure 3.23: Dynamic skin in production wells VMB8 and VMB22 of Washington-Taylorstown field

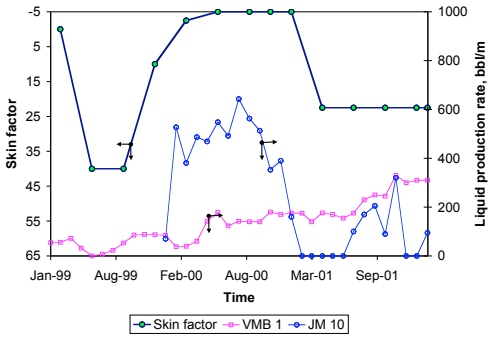

Figure 3.24: Dynamic skin in production wells VMB1 and JM10 of Washington-Taylorstown field

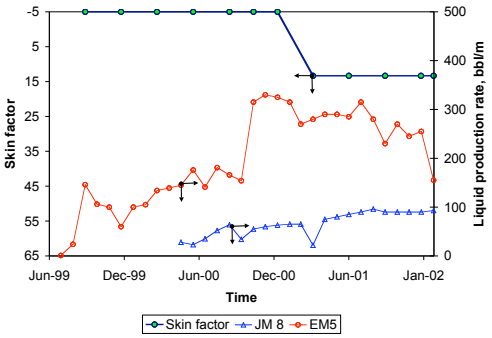

Figure 3.25: Dynamic skin in production wells JM8 and EM5 of Washington-Taylorstown field

4.0 SUMMARY AND CONCLUSION

The objectives of this study were to detail efforts and techniques used to develop representative reservoir models and to provide guidelines for approaching history matching when model development is undertaken using sparse data sets. These objectives were achieved. Using sparse data sets, the reservoir models developed satisfactorily matched the behavior of the reservoirs studied. This suggests that the techniques for characterizing rock and fluid properties were appropriate.

The similarities in the rock and fluid properties for the Taylorstown and the Wileyville reservoirs suggest that data used to characterize and initialize these properties could be extended for use in simulation studies of other reservoirs in the basin. Therefore, this study provides other operators with a tool for analyzing other Gordon reservoirs in the Appalachian basin.

This study shows that the rock properties could be considered uniform throughout the thickness of the reservoirs analyzed. Even though, some log analyses indicated that these reservoirs contain shales forming discontinuities and restrictions to the flow of the different phases, the results obtained suggest that the effect of these shales could be captured by varying the permeability assigned to each block in the models, and that a single layer model is a reasonable approach. These restrictions to the flow suggest that compartmentalization affects the behavior of the reservoir, and may be described in the models using permeability changes in the blocks. It can be concluded that the reservoirs studied may be appropriately described as being heterogeneous single layered.

Given the sparsity of the data, the role of the field staff proved to be crucial in determining the "acceptable" range for adjustment of the reservoir data, and for defining the "confidence" intervals for production data. In addition, the operations staff provided useful insights on the reservoirs. The field staff identified the locations of high water or gas saturations, the location of restrictions to fluid flow in the reservoirs, and reported the operating status of wells that have use for future production or injection. The use of this data improved the "quality" of the history match by incorporating this field knowledge into the process, and thus avoiding a possible numerical solution that does not represent the behavior of the fields.

The systematic approach proposed to complete the history matching proved to be effective in developing an understanding of the behavior of the reservoirs studied. This approach also permitted estimation of the localized damage found in the injection and production wells of the fields.

The results of the study applied to the Taylorstown and the Wileyville fields suggest that the skin damage of all the injection wells increased with time. The formation of emulsions due to the mixture of multiple kinds of injection waters and minerals, the deposition of solids from the injected waters, and the iron precipitate in the borehole due to corrosion of the tubing and casing are the possible causes of the increasing skin damage. Quantification of these effects could not be computed; but were determined inferentially through history matching.

The waterflood operations of the Taylorstown field were evaluated, and predictions of the future behavior of these fields under various operating conditions determined. The following conclusions can be drawn from the reservoir study conducted:

1. The results of the history matching showed that the injection pilot flood exerted an important effect in the southern part of the unit, filling up void spaces and displacing the oil toward the southern portion of the reservoir. The water volumes injected during the injection pilot explain the high fluid levels found in the James Hodgens Sr. 9, and James Hodgens Sr. 10 wells at the beginning of the water injection operations in 1996. It also explained the behavior of J. A. Flack 1 well (JAF 1). This well is located in the southwestern portion of the unit and is the most productive wells in terms of liquid production.
2. The high gas saturation estimated for the northern part of the unit explains the low productivity of the wells, the low oil saturations, and large fill up time for this part of the reservoir.

The objective of the study, which was to analyze the dynamic nature of skin damage, was achieved. The presence of skin is not only due to matrix permeability variations; but also external factors such as mixed fluids injection, suspended particles and particle deposition. In the field case presented in this study, it

was not possible to quantify the impact of each element on well performance and the change of skin with time. The overall skin effect however resulted from:

- Particle deposition. The damage caused by particle deposition appears to be irreversible. It can be reduced through stimulation but original reservoir conditions or zero skin cannot be attained.
- The presence of oxygen in reservoir promotes the formation of skin. Chemical reactions take place in the reservoir and results in the formation of emulsion that causes partial blockage.
- With the presence of oxygen, the oxidation of metallic elements is enhanced and migrates to the formation via transport by injected liquids.

Estimates of the skin can be determined from the rate of change in the injection or production flow rates. This information can be used to optimally schedule well workovers. The results of the study suggest that the more homogeneous the reservoir rock, the greater the benefit of well stimulation reducing near wellbore damage.

Recommendations

It is recommended that field monitoring be continued to confirm the results of this study. The continuous tracking of the behavior of the skin with time will provide a better understanding of its effect with time. This needs to be accomplished not only at the field level, but should include laboratory analysis of the fluids produced.

For studies of other fields in the Appalachian basin, it is recommended that the field operations staff and the simulation team work in concert. The role of the field staff proved to be important in determining the “acceptable” range for adjustment of the reservoir data, and to define the “confidence” intervals for the production data that need to be history matched. In addition, the use of the data provided by the field staff improves the “quality” of the history match by incorporating field knowledge into the solution. This avoids a numerical solution of the problem that might not represent the behavior of the fields.

It is recommended that a chemical analysis of the emulsions that are being recovered during the workovers of the production wells be undertaken. This may allow the identification of a chemical agent that could be injected into the reservoir to improve its injectivity and also reduce the time between workovers.

The evaluation of the waterflood operations and the forecasts performed for the Taylorstown field suggests the following strategies to improve the productivity of the reservoir:

1. Recondition the production wells J.A. Flack 2 (JAF 2), J. A. Flack 3 (JAF 3), James Hodgens Sr. 9 (JHSR 9), James Hodgens Sr. 10 (JHSR 10), T. Hilton 5 (TH 5), and J. Crossland 2 (JC 2) to operate by December 2002.
2. Recondition an injection well of the injection pilot by December 2002.
3. If the results of the wells reconditioned in December 2002 are positive, and in good agreement with the forecast, then it is suggested that consideration be given to the reconditioning of production wells J. Flack 4 (JAF 4), and Carson Heirs 1 (CH 1), which are located outside the unit.
4. Recondition Wells James McMannis 6 (JM 6), H. Westfall Etux 14 (HW 14), and Joseph Hutchinson 5 (JH 5) for operation by August 2004.
5. If the oil and water production is according to the forecast, then it is suggested that two wells be drilled and cored to increase knowledge concerning water and gas saturations in the southern portion of the reservoir. These data are required to evaluate the potential of the possible future expansion of the waterflooding operations.

5.0 REFERENCES

Ahmed, T., 1989, Hydrocarbon Phase behavior: Gulf Publishing Company, Houston, Texas.

Aziz, K., and Settari, A., 1979, Petroleum Reservoir Simulation: Applied Science publishers, pp. 13 - 17.

Aziz, K., 1984, Ten Golden Rules for Simulation Engineers: Journal of Petroleum Technology, p.p. 1157, November 1984.

Beggs, H. D., and Brill, J. P., 1973, A Study of Two-Phase Flow in Inclined Pipes: Journal of Petroleum technology, 607 – 617, May 1973

Beggs, H. D., and Robinson, J. R., 1975, Estimating the Viscosity of Crude Oil Systems: Journal of Petroleum technology, 1140 – 1141, September 1975.

Best, K. D., 2002, Development of an Integrated Model for Compaction/Water Driven Reservoirs and its Application to the J1 and J2 sands at Bullwinkle, Green Canyon Block 65, Deepwater Gulf of Mexico: The Pennsylvania State University, M.S. Thesis.

Brown, G. G., Katz, D. L., Oberfell, C. G., and Alden, R. C., 1948, Natural Gasoline and the Volatile Hydrocarbons: NGAA, Tulsa, OK.

Carr, N. L., Kobayashi, R., and Burrows, D. B., 1954, Viscosity of Hydrocarbon Gases Under pressure: Trans. AIME, 201, 264 – 272, 1954.

Core laboratories, 1981, Special Core Analysis Study for Pennzoil Exploration and Production Company, John McMannis 01 Well, Washington County, PA.

Core laboratories, 1996, Advanced Rock Properties Study L.S. Hoyt No. 100 well. Gordon Sand, Wetzel County, West Virginia, Final Report.

Craft, B. C., and Hawkins M., 1991, Applied petroleum Reservoir Engineering: Prentice Hall, second edition, New Jersey.

Craig, F. F., 1993, The Reservoir Engineering Aspects of Waterflooding: Society of Petroleum Engineers, Monograph volume 3 of the Henry L. Doherty Series, Dallas, TX, January 1993

Damayanti, M. C., 1995, History Matching and Geostatistical Parametric study of a Pilot Area in the Griffithsville Oil Field: The Pennsylvania State University, M.S. Thesis.

Ertekin, T., Abou-Kassem, J. H., and King, G. R., 2001, Basic Applied Reservoir Simulation: Society of Petroleum Engineers Inc., Richardson, TX, pp 22 - 26.

Fanchi, J. R., 1997, Principles of Applied Reservoir Simulation: Gulf Publishing Company, Houston, Texas.

Farias, M. J., 2002, Evaluation of Dynamic Skin as a Part of Waterflooding Analysis: the Pennsylvania State University, M.S. Thesis.

Glaso, O., 1980, Generalized Pressure-Volume-Temperature Correlations: Society of Petroleum Engineers, SPE paper 8016, Dallas, Texas.

Iqbal, G. M., Civan, F., 1993, Simulation of Skin effects and Liquid Cleanup in Hydraulically Fractured Wells: SPE paper 25482, Presented at the Productions Operations Symposium held in Oklahoma City, OK, March 21 – 23.

MacMillan, D. J., Pletcher, J. L., Bourgeois, S. A., 1999, Practical Tools To Assist History Matching: SPE paper 51888, Presented at the 1999 SPE Reservoir Simulation Symposium held in Houston, Texas, February 14 - 17.

Makhlouf, E. M., Chen, W. H., Wasserman, M. L., and Seinfeld, J. H., 1990, A General History Matching Algorithm for Three-Phase, Three-Dimensional Petroleum Reservoirs: SPE paper 20383.

Mattax, C. C., Dalton, R. L., 1990, Reservoir Simulation: Journal of Petroleum Technology (June), vol. 42, No. 6, pp. 692 - 695.

Mattax, C. C., Dalton, R. L., 1990, Reservoir Simulation: Society of Petroleum Engineers, monograph volume 13, Henry L. Doherty series, Richardson, TX.

Meehan, D. N., 1980, A correlation for water compressibility: Petroleum Engineer, p.p. 125 – 126, November 1980.

Parish, R. G., Watkins, A. J., and Muggeridge, A. H., 1993, Effective History Matching: The Application of Advanced Software Techniques to the History matching process, SPE paper 25250.

Peaceman, D. W., 1977, Fundamentals of Numerical Reservoir Simulation: Elsevier Scientific Publishing Company, volume 6.

Standing, M. B., 1977, Volumetric and phase behavior of oil field hydrocarbon systems: Society of Petroleum Engineers of AIME, Dallas, Texas.

Standing, M. B., and Katz, D. L., 1942, Density of Natural Gases: Trans., AIME (1946) 146, 140.

Taber, J. J., Martin, F. D., and Seright, R. S., 1997, EOR Screening Criteria Revisited - Part 1: Introduction to Screening Criteria and Enhanced Recovery Field projects: paper SPE 35385, Presented at the 1996 SPE/DOE Improved Oil Recovery Symposium held in Tulsa, Oklahoma, April 21 - 24.

Thomas, G. W., 1990, History Matching and Other Frustrations: Lectures on Third International Forum on Reservoir Simulation, Austria.

Tippie, D. B., and Van Poolen, H. K., 1974, Variation of Skin Damage with Flow rate Associated with Sand Flow or Stability in Unconsolidated-Sand reservoirs: SPE paper 4886, Presented at the 44th Annual California Regional meeting of the SPE of AIME, held in San Francisco, CA, April 4 - 5.

Vazquez, M., and Beggs, H. D., 1990, Correlations for Fluid Physical Property Predictions: Journal of Petroleum Technology, p.p. 968 – 970, June 1990.

Willhite, G. P., 1986, Waterflooding: Society of Petroleum Engineers, SPE Textbook Series Vol. 3, Richardson, TX.

Yamada, T., 2000, Non-Uniqueness of History Matching: paper 59434, presented at the SPE Asia Pacific Conference on Integrated Modeling for Asset Management held in Yokohama, Japan, April 25-26.